Antiferroelectric and ferroelectric orderings in frustrated chiral tilted smectics and a continuous change from anticlinic SmC_A^* to synclinic SmC^*

2010 EPL 90 56005

(http://iopscience.iop.org/0295-5075/90/5/56005)

A Letters Journal Exploring the Frontiers of Physics

June 2010

EPL, **90** (2010) 56005
doi: 10.1209/0295-5075/90/56005

www.epljournal.org

Antiferroelectric and ferroelectric orderings in frustrated chiral tilted smectics and a continuous change from anticlinic SmC^*_A to synclinic SmC^*

K. L. Sandhya[1], A. D. L. Chandani-Perera[1,2], Atsuo Fukuda[1], J. K. Vij[1(a)] and Ken Ishikawa[3]

[1] *Department of Electronic and Electrical Engineering, Trinity College, University of Dublin - Dublin 2, Ireland, EU*
[2] *Department of Chemistry, Faculty of Science, University of Peradeniya - Peradeniya, Sri Lanka*
[3] *Department of Organic and Polymeric Materials, Tokyo Institute of Technology - Tokyo 152-8552, Japan*

received 30 April 2010; accepted in final form 7 June 2010
published online 6 July 2010

PACS 61.30.Eb – Experimental determinations of smectic, nematic, cholesteric, and other structures
PACS 64.70.M- – Transitions in liquid crystals
PACS 77.80.-e – Ferroelectricity and antiferroelectricity

Abstract – In a frustrated binary-mixture system of ferroelectric and antiferroelectric liquid crystals, where the border line between SmC^*_A and SmC^* in the temperature-concentration phase diagram runs almost parallel to the ordinate temperature axis, we have found a continuous change between them close to the critical concentration. The continuity has been confirmed as an intrinsic property in the bulk by observing almost perfect bell-shaped Bragg reflection bands due to the helicoidal director structure. The temperature variation of peak wavelength of the half-pitch band and, in particular, the characteristic disappearance of the full-pitch band apparently within the SmC^* temperature region have been simulated with a change in the ratio of ferroelectric and antiferroelectric orderings. The observed continuous change has been described by the entropy effect in the 1D Ising model with the synclinic and anticlinic orderings as spins.

Ordinary tilted smectic liquid crystals consist of rodlike molecules that are aligned to form a stack of 2D liquid layers with a thickness, l, of an order of the rod length. The average orientation of long molecular axes (the director $\mathbf{n}_i$) in the i-th smectic layer is described by a tilt angle, θ_i, to the layer normal $\mathbf{k}$ and an azimuthal orientation, φ_i. Here θ_i is constant throughout the bulk sample, and the layer-to-layer progression of φ_i distinguishes various phases. Two main phases are smectic-C, (SmC), and smectic-C_A, (SmC_A). These are characterized by the synclinc ($\Delta\varphi \equiv \varphi_{i+1} - \varphi_i = 0°$) and the anticlinic ($\Delta\varphi = 180°$) orderings, respectively, throughout the bulk. When the system is chiral, these phases are designated as ferroelectric SmC^* and antiferroelectric SmC^*_A; each layer has the spontaneous polarization, $\mathbf{P}_i \propto \mathbf{k} \times \mathbf{n}_i$. The chirality leads to additional small modulations in the azimuthal angle, $\Delta\varphi = \delta_C$ in SmC^* and $\Delta\varphi = 180° + \delta_{CA}$ in SmC^*_A. Here δ_C and δ_{CA} are both ca. 1° and have opposite signs; the helicoidal full pitches, $p_C = (360/\delta_C)l$ and $p_{CA} = (360/\delta_{CA})l$, typically encompass hundreds of layers and may produce the Bragg reflections in the optical wavelength region. Since the ferroelectric and antiferroelectric orderings are almost synclinic and anticlinic, respectively, the helicoidal periodicity is the full pitch in SmC^* whereas it is the half pitch in SmC^*_A. Consequently, the Brillouin zones are $\pm\pi/p_C$ and $\pm\pi/(p_{CA}/2)$, respectively; the 2nd-order, ordinary characteristic reflections (the half-pitch bands) are observed in both phases, but the 1st-order, total reflection (the full-pitch band) appears only in SmC^* [1,2].

In many antiferroelectric liquid crystals (AFLCs), the phase transition occurs directly between SmC^*_A and SmC^*. A large number of alternative superstructures characterized by the mixture of the ferroelectric and antiferroelectric orderings have the same free energy at the transition temperature (the frustration point). When the short-range interlayer interactions between adjacent layers alone are operative, however, none of the superstructures thus produced has a lower free energy than that of SmC^*_A or SmC^* [3]. The transition is of 1st order and occurs inhomogeneously through the propagation of solitary waves, which are the boundaries

(a) E-mail: jvij@tcd.ie

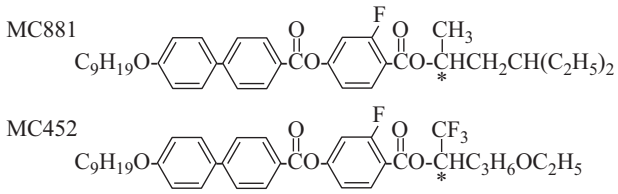

Fig. 1: The chemical structures of MC881 and MC452, both of which are (*R*)-moieties.

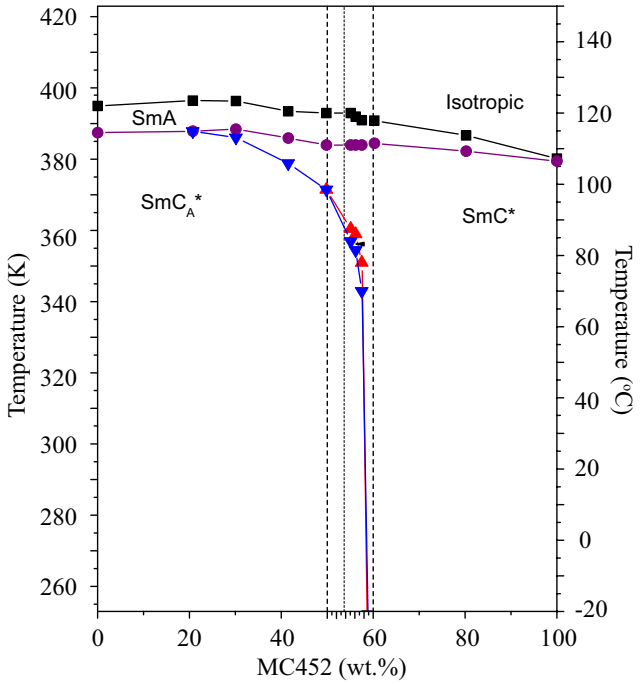

Fig. 2: (Colour on-line) The global temperature-concentration (*T*-*r*) phase diagram for a binary-mixture system of antiferroelectric MC881 and ferroelectric MC452. The boundary between SmC^*_A and SmC^* becomes blurred for MC452 concentrations higher than 50 wt.%. In ref. [19], the blurring was ascribed to the emergence of Sm$C^*_A(1/3)$, but the present study clarifies continuous changes, indicating that Sm$C^*_A(1/3)$ does not stably exist at zero electric field. For details see text.

between macroscopic SmC^*_A and SmC^* domains [4,5]. Any long-range interlayer interactions (LRILIs) may lift the degeneracy and stabilize some of the superstructures to exist as subphases in finite temperature ranges [3]. So far as we are aware of, three reasonable theoretical models for the LRILIs have been proposed, which can predict the emergence of subphases other than the typical ones with 3- and 4-layer superstructures [6–9]. Among them, the Emelyanenko-Osipov model can intuitively explain the microscopic short-pitch helical structures, though highly distorted, of the subphases as well as the staircase character of the subphase emergence, both of which were experimentally confirmed unambiguously [10–16].

The subphase superstructures are still specified by $q_T = [F]/([A]+[F])$ as originally done on the basis of the Ising model, if $[F]$ and $[A]$ are re-interpreted as the

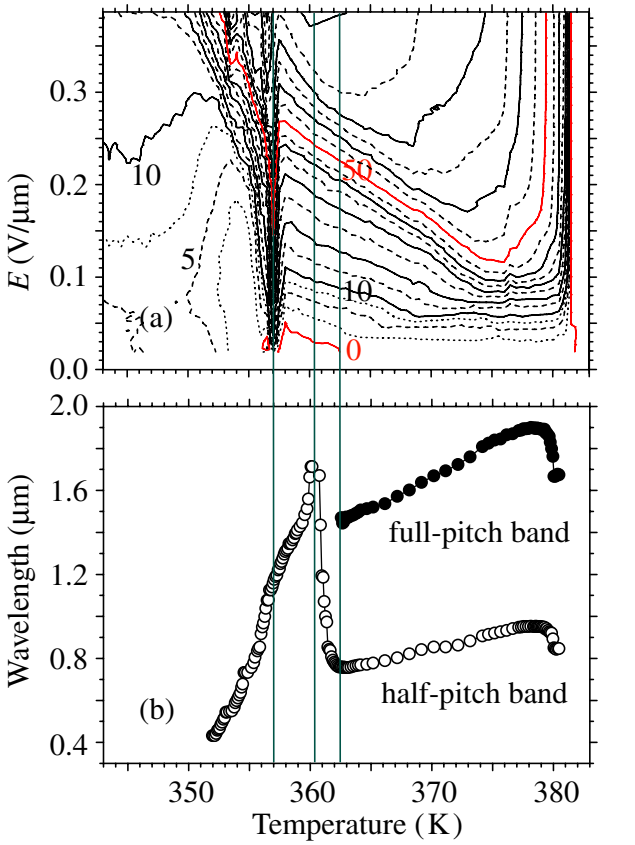

Fig. 3: (Colour on-line) (a) *E*-*T* phase diagram with field-induced birefringence contours in a 25 μm homeotropic cell. Marked are the values of birefringence Δn multiplied by 10^{-3}. The contour lines are drawn at a step of $\Delta n = 5\times10^{-3}$, and (b) temperature variation of the Bragg reflection peaks, in a binary mixture of MC881 containing 53.74 wt.% MC452.

numbers of *quasi*-synclinic ferroelectric and *quasi*-anticlinic antiferroelectric orderings in a unit cell, respectively [10,17]. Since these LRILIs are generally weak, the lower-temperature subphase is expected to have a smaller q_T than the higher-temperature one. In fact, subphases with $q_T = 1/4$, $1/3$, $2/5$, $1/2$, $3/5$ and $2/3$ have been reported to emerge in the order of increasing temperature; the 3-, 4- and 6-layer superstructures with $q_T = 1/3$, $1/2$ and $2/3$, Sm$C^*_A(1/3)$, Sm$C^*_A(1/2)$ and SmC^*_{d6}, have been well confirmed by sophisticated experimental techniques [10–16]. Here the subphase with $q_T = 2/3$ is designated as SmC^*_{d6} by specifying the distorted microscopic helical short-pitch, p_{qT} [16]. In fact we reported an additional phase with a number of layers in a unit cell either 5 or 6 [10] prior to the work of Wang *et al.* [16]. The exact number of layers in the unit cell could not have been confirmed at that stage. In the Emelyanenko-Osipov model, the pitch is generally given by

$$|\,p_{qT}\,| = \frac{2}{1-q_T}. \qquad (1)$$

Since the subphase superstructure is approximately characterized by the mixture of the synclinic and anticlinic

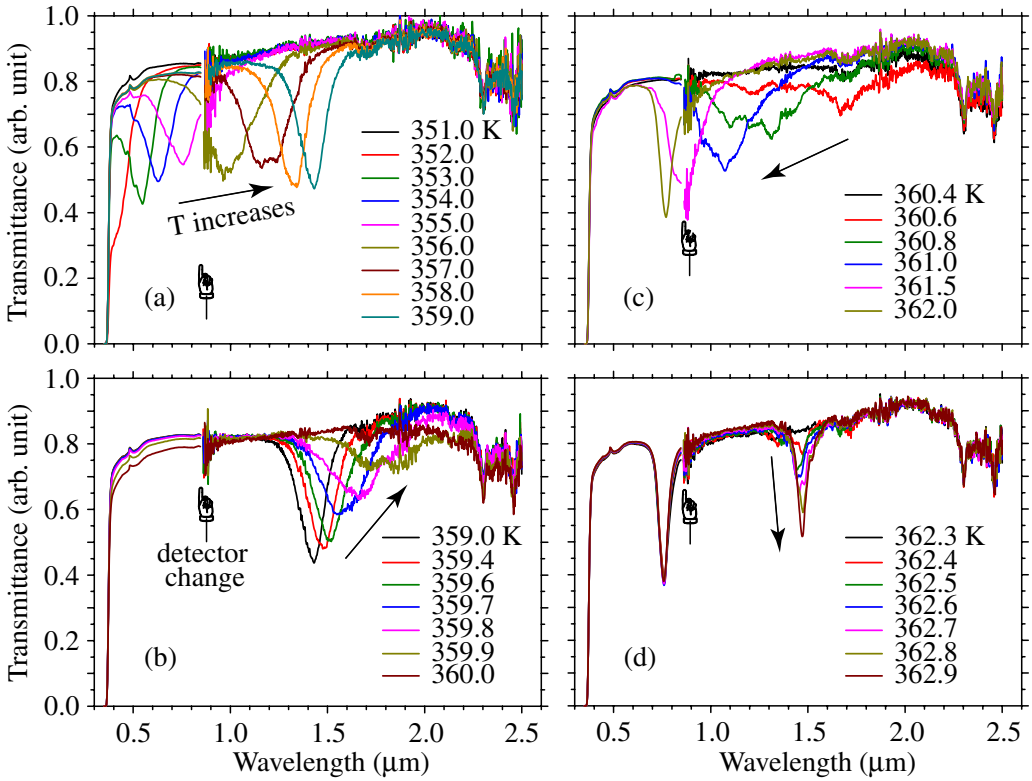

Fig. 4: (Colour on-line) Typical continuous change from SmC^*_A to SmC^* observed in a binary mixture of MC881 containing 53.74 wt.% MC452: some of the transmittance spectra measured at 20° oblique incidence by raising temperature at intervals of 0.1°C in a 50 μm homeotropic cell. The absorption peaks in the transmittance spectra correspond to the Bragg reflection peaks.

orderings, the macroscopic helical pitch of the subphase with q_T, $p(\mathrm{Sm}C^*_A(q_T))$, is given approximately by

$$\frac{1}{p(\mathrm{Sm}C^*_A(q_T))} = \frac{q_T}{p(\mathrm{Sm}C^*)} + \frac{1-q_T}{p(\mathrm{Sm}C^*_A)}, \qquad (2)$$

where $p(\mathrm{Sm}C^*)$ and $p(\mathrm{Sm}C^*_A)$ have opposite signs [10,13,18].

In this way, not only the direct transition between SmC^*_A and SmC^* but the sequential transitions as well via the subphases are of 1st order and these accompany abrupt changes in the macroscopic helicoidal pitch. Recently, however, we encountered an unexpected, very special AFLC where the change from SmC^*_A to SmC^* is continuous in the sense that the macroscopic helicoidal pitch does not show any abrupt jump. The AFLC is a binary-mixture system of antiferroelectric MC881 and ferroelectric MC452, the chemical structures of which are given in fig. 1. The global temperature-concentration (T-r) phase diagram has been roughly obtained as reproduced in fig. 2 [19]; the border line between SmC^*_A and SmC^* runs almost parallel to the ordinate temperature axis so that we can define the critical concentration, r_c. Among the several mixtures near r_c that were studied, we report here the details of a MC881 mixture containing 53.74 wt.% MC452, which shows a most typical continuous change and conclude that it results from the lifting of degeneracy due to the entropy effect. Note that the continuous change at issue is an intrinsic property observed in the bulk and hence this is completely different from the "Gradual phase transition…" treated in ref. [19] which in turn is caused by the interface effect. The Bragg reflection bands were obtained by measuring the transmittance spectra at an oblique angle of incidence of 20°; the full-pitch band could not be observed for normal incidence because of the selection rule. In order to check whether there do exist any subphases, we also obtained the E-T phase diagram by drawing the contour lines of electric-field-induced birefringence which was measured using a photoelastic modulator (PEM). The contours show characteristic patterns indicating the stability of the subphases as well as the main phases, SmC^*_A, SmC^*, and SmA, under electric field [10].

Figure 3(a) is the E-T phase diagram and has such characteristic patterns. The contour lines show a valley (the most easily deformable region) at around 357.0 K, which indicates that an applied electric field stabilizes Sm$C^*_A(1/3)$. Since the bottom of the valley is not flat but sharp-pointed downwards, however, Sm$C^*_A(1/3)$ does not stably exist at zero field. Such a situation has been observed in several compounds and mixtures recently [10]. There also seem to emerge SmC^* (358.0–381.0 K) and SmA (above 382.0 K) on the high-temperature side and SmC^*_A on the low-temperature side. Moreover, the behavior of the contour lines just below Sm$C^*_A(1/3)$ seems to indicate the possible emergence of several subphases,

Sm$C_A^*(0 < q_T < 1/3)$'s. Figure 3(b) shows the Bragg reflection peaks *vs.* temperature. We observe no reflection band in the SmC_A^* temperature region because, as the concentration of MC452 increases, the reflection band moves toward the shorter-wavelength side and comes to be buried in the intrinsic absorption even in the ca. 10 wt.% mixture; the half-pitch band in SmC_A^* of pure MC881 is observed at about 0.4 μm with right-handed circular polarization for normal incidence. Figure 4(a)–(d) illustrates some of the transmittance spectra. The reflection band is almost completely buried under the intrinsic absorption at 351.0 K, this shows a shoulder at 352.0 K and a peak at 353.0 K is clearly observed as seen in fig. 4(a). As the temperature increases further, the reflection band moves toward the longer-wavelength side; it broadens slightly when the peak-temperature curve shows a bulge and then becomes slightly sharper at around 358.0–359.0 K as seen in fig. 3(b) and fig. 4(a). The bulge consisting of slightly broader reflection bands must be related with Sm$C_A^*(1/3)$; nevertheless, the macroscopic helicoidal pitch changes continuously across the subphase region.

On a further increase in the temperature, the peak wavelength and the band width abruptly increase at the same time as shown in fig. 3(b) and fig. 4(b). Although no reflection band is observed between 360.2 and 360.6 K in the wavelength region covered by the spectrometer used, though very noisy above 1.6 μm, a very broad reflection band is observed at 360.6 K again. Then the peak wavelength and the band width abruptly decrease at the same time up to ca. 362.3 K as seen in fig. 3(b) and fig. 4(c). The peak wavelength appears to diverge at 360.4 K; the reflection band is right circularly polarized on the low-temperature side of the divergence while left circularly polarized on the high-temperature side. Note that the divergence occurs in the apparent SmC^* temperature region (358.0–381.0 K) as assigned above from the observed characteristic patterns of the contour lines in the *E*-*T* phase diagram. So long as the full-pitch band is observed, the phase can be assigned as SmC^*; however, the full-pitch band is not observed below 362.3 K. By increasing the temperature above 362.3 K, the full-pitch band emerges and its intensity increases continuously until 363.0 K; contrastingly, the half-pitch band does not show any change during the building-up process of the full-pitch band as seen in fig. 4(d). Afterwards both bell-shaped full- and half-pitch bands move slightly toward the longer-wavelength side, and then at 379.0 K they show rather steep decreases in the peak wavelengths. These slight gradual increases and sudden decreases in the peak wavelengths are frequently observed and are considered to be the characteristic features of SmC^* [10,18].

An increase in the peak wavelength accompanied with a broadening of the reflection band interlaced with multipeaks were observed just above SmC_A^* in some other AFLCs. These observations were ascribed to an emergence of several subphases just above SmC_A^*,

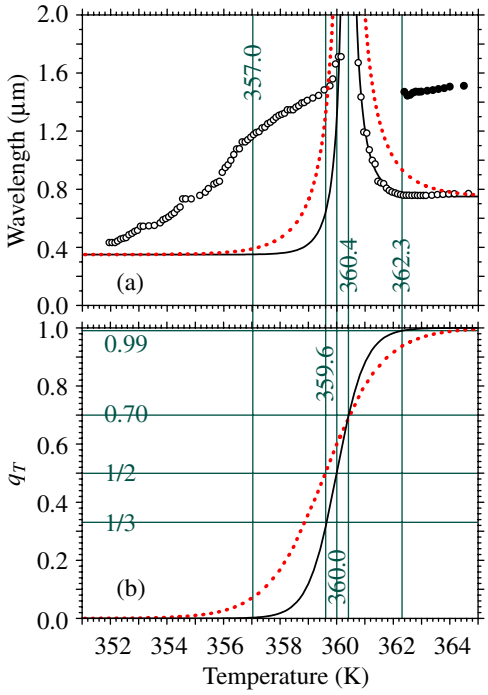

Fig. 5: (Colour on-line) (a) Bragg reflection peak and (b) ratio of ferroelectric ordering in a unit cell q_T are plotted as functions of temperature T using eqs. (2) and (3). The observed temperature change given by open circles is rather well reproduced on the high-temperature side with $T_c = 360.0$ K and $\alpha/k_BT^* = 2.0$. For reference, a curve with 359.6 K and 1.0 is also drawn by red dotted lines.

Sm$C_A^*(0 < q_T < 1/3)$'s, due to the LRILIs [6,10]. However, the experimental results presented in figs. 3 and 4 for the 53.74 wt.% mixture are characteristically different from those reported previously such that the peak wavelength of the reflection band changes continuously over a wide range of wavelengths varying from 0.35 μm to 1.7 μm, crossing the bulge in the Sm$C_A^*(1/3)$ region. In addition the reflection band keeps its almost bell-shaped appearance throughout the range of wavelengths. In a similar manner, on the high-temperature side, a conspicuous decrease in the peak wavelength and a sharpening of the reflection band cannot be ascribed to an emergence of several subphases with $1/3 < q_T < 1$ due to some sort of LRILIs, either. Among the three theoretical models for the LRILIs proposed, so far, in the literature which can explain the emergence of subphases other than the typical ones with 3- and 4-layer superstructures, Sm$C_A^*(1/3)$ and Sm$C_A^*(1/2)$, no model predicts the emergence of *several* subphases, Sm$C_A^*(1/3 < q_T < 1)$'s, on the high-temperature side of Sm$C_A^*(1/3)$ [6–9]. We need to find out another cause for the observed continuous change in the macroscopic helicoidal pitch from SmC_A^* to SmC^*. Since the energy difference between SmC^* and SmC_A^* in the 53.74 wt.% mixture must be appreciably small over a very wide temperature range [19], let us examine as to what extent the entropy effect in the lifting of degeneracy

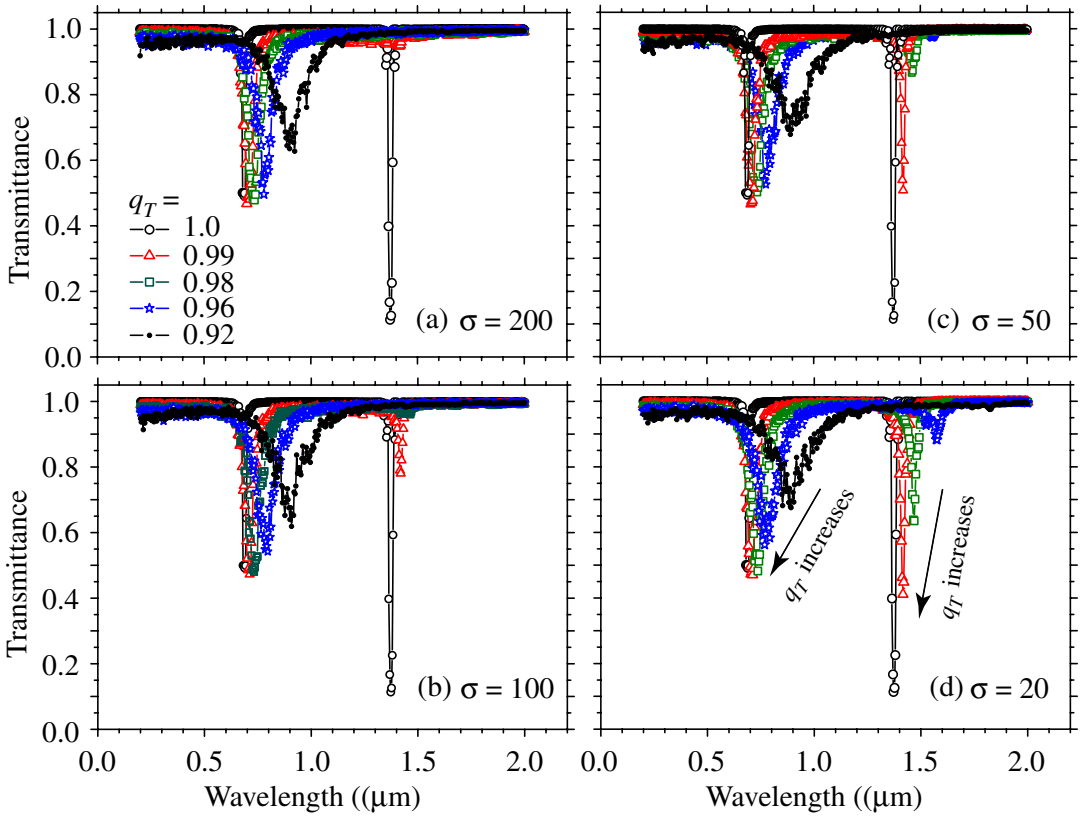

Fig. 6: (Colour on-line) Some spectra for half- and full-pitch bands are calculated by randomly distributing paired anticlinic-ordering defects in the otherwise synclinic ordering prevailing throughout the bulk with 15000 smectic layers. The defect separation of a pair is characterized by the normal distribution with a standard deviation of σ layers. The number of layers contained in the full pitch is 62 for SmC_A^* and 140 for SmC^* with a layer thickness of 3.5 nm.

at the frustration point can explain the experimental results given above [20].

The change between SmC_A^* and SmC^* is usually considered to occur through the azimuthal angle freedom, but the energy barrier between them is expected to be very large even in the 53.74 wt.% mixture [19]. The entropy effect can be treated in the 1D Ising model with the synclinic and anticlinic orderings as spins, where the continuous change but not the phase transition is to occur. The energy difference can be approximated as $\Delta E = E_{CA} - E_C \simeq \alpha\,(T - T_c)$, where $\alpha > 0$ is a constant and T_c the virtual phase transition temperature between SmC_A^* and SmC^*. On assuming that the ratio of $[A]$ to $[F]$ is given by the Boltzmann distribution with an effective temperature $T^* \ll T_c$, we obtain

$$q_T = \frac{1}{1 + \exp\{-(\alpha/k_B)(T - T_c)/T^*\}}, \qquad (3)$$

where use is made of the definition of q_T. By combining eqs. (2) and (3) and by ignoring the dispersion of refraction indexes, the experimentally observed Bragg reflection peak vs. temperature, at least on the high-temperature side of the pitch divergence at $T = 360.4$ K ($q_T = 0.70$), is rather well reproduced as shown in fig. 5. We assume the half-pitch reflection bands occur at 0.35 and 0.75 μm in SmC_A^* and SmC^*, respectively, disregarding the temperature variation within the main phases. The handedness changes from right to left when crossing the divergence with increasing temperature. An appreciable increase in the peak wavelength can be seen at $q_T = 0.9$ but not at $q_T = 0.99$.

In order to see to what extent the entropy effect can explain the continuous build-up of the full-pitch band at around 362.3 K, let us simulate the Bragg reflection bands by assuming appropriate superstructures with $q_T = 0.9$–0.99. Thermally induced flip-flopping between the synclinc and anticlinic orderings may occur through a simultaneous change in the tilting sense of some neighboring layers with a solitary wave propagation; anticlinic ordering defects are dynamically created or annihilated as pairs in the otherwise synclinic ordering prevailing throughout the bulk. Some LRILIs may also promote defect movements along the layer normal direction. The defect pairs must be distributed randomly throughout the bulk and their average number is $(1 - q_T)/2$, which is given above as a function of T. The only parameter necessary to simulate the superstructure at T is the defect separation of a pair, $n = \lfloor |x| \rfloor + 1$ smectic layers, where x is assumed to be given by random numbers distributed normally with a standard deviation of σ smectic

layers, $\exp\{-x^2/(2\sigma^2)\}/(\sqrt{2\pi}\sigma)$. We have calculated the Bragg reflection spectra by using Berreman's 4×4 matrix method for randomly produced 10 superstructures and then have averaged them out. Figure 6 summarizes the results, which successfully reproduce the disappearance of the full-pitch band within the apparent SmC^* temperature region, although a rather large σ needs to assure the disappearance at around $q_T \simeq 0.99$. In spite of the success in the high-temperature region, eqs. (2) and (3) could hardly reproduce the experimentally observed continuous temperature variation of the Bragg reflection peak in the low-temperature region. The interplay between the entropy effect and the LRILIs must be important and is an interesting problem to be studied in the near future.

Is it possible that the synclinic and anticlinic orderings are flip-flopping dynamically in the 53.74 wt.% mixture and if so why? The well-established tilted smectic structure suppresses the thermal excitation of the cooperative director motion of the antiphase mode, the latter promotes the change between SmC_A^* and SmC^*; hence the phase transition between them is ordinarily treated in the absolute-zero-temperature approximation by neglecting the entropy effect. It is not impertinent, however, to conclude that the observed thermally induced continuous change from SmC_A^* to SmC^* near the critical concentration, r_c, is due to the lifting of degeneracy at the frustration point arising from the entropy effect because of an exceptionally small α. In fact, Song *et al.* studied the field-induced phase transition from SmC_A^* to SmC^* in the 20–50 wt.% mixtures, determined α, and confirmed that it rapidly becomes smaller as the MC452 concentration approaches the critical concentration, $r_c \simeq 59$ wt.% [19]. They obtained $\alpha = 2.5\times10^3\,\mathrm{erg\cdot cm^{-3}\cdot K^{-1}}$ in the 50 wt.% mixture. This corresponds to $5\times10^4\,\mathrm{erg\cdot cm^{-3}}$ at $T - T_c = 20$ K and which is three orders of magnitude smaller than the thermal energy k_BT/(volume per molecule) at 300 K. Note that the dynamical flip-flopping of a smectic layer has been known to show a very slow relaxation, 132 Hz, in the autocorrelation of the laser beam diffraction intensity observed in Sm$C_A^*(1/3)$ of MHPOBC [21]. It is suggested that the photon correlation spectroscopy experiment on the 53.74 wt.% mixture must be useful in elucidating the details of the dynamical flip-flopping processes.

* * *

Mitsubishi Gas Chemical Company, Inc. is acknowledged for the gift of liquid-crystal compounds, and the Irish Research Council of Science Engineering and Technology is thanked for the award of a post-doctoral Fellowship to KLS. The laboratory facilities were equipped with a grant from SFI.

REFERENCES

[1] Meyer R. B., Liebert L., Strzelecki L. and Keller P., *J. Phys. (Paris), Lett.*, **36** (1975) L69.
[2] Chandani A. D. L., Gorecka E., Ouchi Y., Takezoe H. and Fukuda A., *Jpn. J. Appl. Phys., Part 2*, **28** (1989) L1265.
[3] Prost J. and Bruinsma R., *Ferroelectrics*, **148** (1993) 25.
[4] Li J.-F., Wang X.-Y., Kangas E., Taylor P. L., Rosenblatt C., Suzuki Y. I. and Cladis P. E., *Phys. Rev. B*, **52** (1995) R13075.
[5] Song J.-K., Fukuda A. and Vij J. K., *Phys. Rev. Lett.*, **101** (2008) 097801.
[6] Emelyanenko A. V. and Osipov M. A., *Phys. Rev. E*, **68** (2003) 051703.
[7] Shtykov N. M., Chandani A. D. L., Emelyanenko A. V., Fukuda A. and Vij J. K., *Phys. Rev. E*, **71** (2005) 021711.
[8] Dolganov P. V., Zhilin V. M., Dolganov V. K. and Kats E. I., *Phys. Rev. E*, **67** (2003) 041716.
[9] Hamaneh M. B. and Taylor P. L., *Phys. Rev. Lett.*, **93** (2004) 167801.
[10] Sandhya K. L., Vij J. K., Fukuda A. and Emelyanenko A. V., *Liq. Cryst.*, **36** (2009) 1101.
[11] Mach P., Pindak R., Levelut A.-M., Barois P., Nguyen H. T., Huang C. C. and Furenlid L., *Phys. Rev. Lett.*, **81** (1998) 1015.
[12] Johnson P. M., Olson D. A., Pankratz S., Nguyen T., Goodby J., Hird M. and Huang C. C., *Phys. Rev. Lett.*, **84** (2000) 4870.
[13] Lagerwall J. P. F., Giesselmann F. and Osipov M., *Liq. Cryst.*, **33** (2006) 625.
[14] Marcerou J. P., Nguyen H. T., Bitri N., Gharbi A., Essid S. and Soltani T., *Eur. Phys. J. E*, **23** (2007) 319.
[15] Jaradat S., Brimicombe P. D., Southern C., Siemianowski S. D., DiMasi E., Osipov M., Pindak R. and Gleeson H. F., *Phys. Rev. E*, **77** (2008) 010701(R).
[16] Wang S., Pan L.-D., Pindak R., Liu Z. Q., Nguyen H. T. and Huang C. C., *Phys. Rev. Lett.*, **104** (2010) 027801.
[17] Fukuda A., Takanishi Y., Isozaki T., Ishikawa K. and Takezoe H., *J. Mater. Chem.*, **4** (1994) 997.
[18] Li J., Takezoe H. and Fukuda A., *Jpn. J. Appl. Phys.*, **30** (1991) 532.
[19] Song J. K., Fukuda A. and Vij J. K., *Phys. Rev. E*, **78** (2008) 041702.
[20] Bak P., *Phys. Today*, **39**, issue No. 12 (1986) 38.
[21] Miyachi K., Kabe M., Ishikawa K., Takezoe H. and Fukuda A., *Ferroelectrics*, **147** (1993) 147.